Journal of Catalysis **188,** 165–175 (1999)
Article ID jcat.1999.2635, available online at http://www.idealibrary.com on IDEAL®

High Performances of Pt/ZnO Catalysts in Selective Hydrogenation of Crotonaldehyde

M. Consonni,* D. Jokic,* D. Yu Murzin,† and R. Touroude*,[1]

*LERCSI, UMR 7515 du CNRS, ECPM, ULP, 25 rue Becquerel, 67087 Strasbourg Cedex 2, France; and †Laboratory of Industrial Chemistry, Abo Akademi, FIN-20500, Turku, Finland

Received May 6, 1999; revised July 1, 1999; accepted July 5, 1999

Hydrogenation of crotonaldehyde in the gas phase, at atmospheric pressure and 353 K over Pt/ZnO catalysts, was studied. Two types of precursor, $(Pt(NH_3)_4(NO_3)_2$ and H_2PtCl_6, referred to as A and B catalysts, respectively, were used for catalyst preparation. Before the catalytic experiments the catalysts were reduced at different temperatures. The reducibility of the support and the catalysts was followed by TPR. Catalysts were also analysed by XPS and XRD. Rapid deactivation during time on stream was observed. The A and B catalysts showed different dependence on the reduction temperature. Thus, the A catalyst had the highest activity when reduced at 473 K; a further increase in the reduction temperature led to a decrease in the activity, but at 673 K both catalysts A and B showed nearly the same activity. On the B catalyst, the crotyl alcohol selectivity reached a value as high as 75–80%, whatever the reduction temperature. The B catalyst was better dispersed than the A catalyst and formed a PtZn alloy at low reduction temperature (473 K). It contained about 5 wt% chloride, whatever the reduction temperature. In contrast, Pt metal particles were only formed on the A catalyst, reduced at 473 K, and then showed low selectivity in crotyl alcohol. However, when the reduction temperature was increased, activity decreased and crotyl alcohol selectivity increased parallel to Pt–Zn alloy formation. One can speculate that Pt sites, when alloyed to Zn, formed $Pt^{\delta-}$–$Zn^{\delta+}$ entities, on which the crotonaldehyde adsorbed by the carbonyl group rather than by the C=C double bond. On the B catalyst, the high selectivity observed, whatever the reduction temperature, led us to assume that besides the alloying effect, chlorine has an important promotor effect by increasing the polarity of $Zn^{\delta+}$ in the PtZn catalytic sites and facilitating the carbonyl adsorption. A reaction network and mechanism were put forward. Kinetic models, developed from the proposed elementary step mechanisms, were used to discuss the influence of support and promoters on reaction selectivity.

Key Words: **platinum; hydrogenation; crotonaldehyde; Pt/ZnO; unsaturated alcohol.**

INTRODUCTION

Hydrogenation is used on a large scale in the chemical and petrochemical industry, the food-processing industry, pharmaceutical production, and fine chemicals (1). One of the challenging tasks, from both scientific and industrial points of view, is selective (chemio-, stereo-, regio-, or enantio-) reduction of polyfunctional molecules taking part in these processes.

Selective hydrogenation of α,β-unsaturated aldehydes is an interesting model reaction because these molecules simultaneously contain C=O and C=C bonds which, moreover, form a conjugated system. So selective reduction of C=O to obtain the unsaturated alcohol while C=C remains unaffected is a difficult task to achieve.

In this field of research, monometallic catalysts supported on Al_2O_3 or SiO_2 lead mostly to the formation of saturated aldehydes (2). To improve selectivity toward unsaturated alcohols, the use of additives (promoters), bimetallic catalysts, or easily reducible supports has been proposed. Different results can be obtained, depending on the nature of the metal itself. The effects of promotion were recently discussed in detail by Ponec (3). Promoters are thought to be needed for the activation of the carbonyl group due to the formation of a chemical bond between the oxygen of this group and the promoter in its cationic state. For crotonaldehyde hydrogenation in the gas phase, much attention has been given to the performance of Pt–Sn catalysts for which the selectivity in unsaturated alcohol was found to depend on the Sn/Pt ratio, the preparation method, and more precisely the Pt–Sn or Pt–Sn oxide interactions (4). Another interesting system is platinum deposited on titania (5–8). It was speculated that after a high-temperature reduction Pt–titania interfacial sites are created, which are responsible for this enhancement.

Besides TiO_2, other reducible oxides such as Nb_2O_5, Y_2O_3, ZrO_2, and CeO_2 used as supports of platinum have been found to contribute to changes in the catalytic activity and selectivity in acrolein (9) and crotonaldehyde (10) hydrogenation. As the selective hydrogenation of crotonaldehyde is known to be a reaction sensitive to metal–support interactions, it was interesting to test the properties of Pt/ZnO catalysts for this reaction, knowing that ZnO has shown promoting effects in several studies. In the water-gas

[1] To whom correspondence should be addressed.

0021-9517/99 $30.00

shift reaction (11) and the methanation of carbon monoxide (12), which were conducted over Pt/ZnO catalysts, the activity increased with the reduction temperature treatment; that was explained by an atomic rearrangement at the metal–semiconductor interface (11) and by a significant ligand effect of Zn in the formed PtZn alloy (12). A marked decrease in the catalytic activity with a significant increase in selectivity was observed in butadiene hydrogenation to olefins when the Pd/ZnO catalyst was reduced above 423 K. It was suggested that Pd crystallites were "decorated" by metallic Zn, leading to less availability of Pd adsorption sites (13). Exceptional performance of Pd/ZnO catalysts in steam reforming reactions, dehydrogenation of methanol into methyl formate (14, 15), and hydrogen production by partial oxidation of methanol (16) has been reported.

This paper is devoted to the hydrogenation of crotonaldehyde in the gas phase on Pt deposited on ZnO, using different metal precursors and different reduction temperatures.

2. EXPERIMENTAL

Catalyst Preparation

Two Pt/ZnO catalysts, A and B, were prepared by wet impregnation of ZnO (Asturienne des Mines, 42.6 $m^2 g^{-1}$ precalcined at 673 K) using aqueous solutions of respectively tetraammineplatinum(II) nitrate ($Pt(NH_3)_4(NO_3)_2$) and hexachloroplatinic acid (H_2PtCl_6); both salt and acid were supplied by Strem Chemicals. The water was slowly eliminated by evaporation on a hot plate. The samples were dried overnight at 383 K, calcined in air at 673 K for 4 h, and stored until use. Atomic absorption analyses (AAS) were performed on the calcined samples (at CNRS, Vernaison, France) to evaluate the metal and chlorine loadings (Table 1).

TABLE 1

Catalyst Description

	A catalyst	B catalyst	ZnO support
Precursor	$Pt(NH_3)_4(NO_3)_2$	H_2PtCl_6	Asturienne des Mines (BET: 42.6 m^2/g)
Pt content (wt%)	5.0	5.0	
		Cl content (wt%)	
Calc. at 673 K	0.016	5.35 (Cl/Pt) atomic = 5.8	0.016
Red. at 473 K		6.49 (Cl/Pt) atomic = 7.1	
Red. at 773 K		5.89 (Cl/Pt) atomic = 6.4	
Red. at 873 K	<0.009	0.21–0.72 (inhomogeneous)	0.013

Catalytic Tests

Catalytic tests were carried out in a glass reactor, operated at atmospheric pressure. The total gas flow, controlled by a flow meter, was varied by changing the pumping rate at the end of the flow line. Crotonaldehyde (CROTAL) supplied by Fluka puriss and stored in argon was used as received. A known quantity of CROTAL (50–200 μL) was drawn up from the bottle using a tight syringe and introduced through a vaccine cap into a reservoir, installed on-line, and maintained at 273 K; therefore, CROTAL at constant partial pressure (8 Torr) was carried over the catalyst by the hydrogen flow (30–40 cc/min). The H_2 gas was first purified by passing it through a trap, maintained at room temperature, containing the Pt/Al_2O_3 catalyst mixed with zeolite to remove oxygen and water. Further purification was made through an MnO trap at 293 K, installed just before the CROTAL reservoir. Beyond the CROTAL reservoir, the gas line was thermostated at about 333 K to avoid any condensation. The stability of the CROTAL pressure and the duration of the experiment were controlled by two catharometers inserted upstream and downstream with respect to the reactor, enabling the CROTAL flow rate (0.22–0.32 μmol s^{-1}) to be measured. The reaction products were drawn off the flow line at different times during the catalytic run and analyzed by gas–liquid chromatography (GLC) with a 30-m long, 0.5461×10^{-3}-m diameter DB-Wax column (J&W Scientific), at 358 K using a flame ionization detector.

Before each catalytic experiment, the catalyst (100–200 mg) was reduced at the desired temperature for 4 h and cooled under H_2 flow to the reaction temperature (353 K).

The reaction activities were calculated using the formula $A = (\alpha F/\omega)$, α being the CROTAL conversion, F the CROTAL flow in mol/s, and ω the weight of platinum in grams. The selectivity to the different products, crotyl alcohol (CROTOL), butanal, butanol, hydrocarbons, and some side products, was calculated as the molar ratio of the selected product to the total products formed. The sensitivity factors are taken as 1 for CROTAL, CROTOL, butanal, butanol, and side products and 1.4 for the hydrocarbons. The identification of the various hydrocarbons and side products was occasionally made using a DB 624 chromatographic column connected to a mass spectrometer (Carlo Erba).

It was checked that ZnO alone had no activity for crotonaldehyde hydrogenation after H_2 pretreatment up to 673 K.

X-Ray Photoelectron Spectroscopy Analysis (XPS)

X-ray photoelectron spectroscopy (XPS) analyses were performed using a VG ESCA III spectrometer with Mg$K\alpha$ radiation (1253.6 eV) as an incident beam without a monochromator. Before the analysis was conducted, the samples were treated at different temperatures at

atmospheric pressure in air or hydrogen in a preparation space connected to the analysis chamber.

To obtain the Pt(4*f*) signals, the deconvolution procedure was applied in the 64- to 99-eV BE range, taking into account the Zn(3*p*) signals and their satellites (due to the Mg$K\alpha 2,\alpha 3$ X-ray excitation source). The Pt($4f^{7/2}$) BE was referred to Zn($3p^{3/2}$) BE at 88.3 eV obtained after the fitting procedure. Theoretical curves were adjusted to fit the peaks by a homemade computer program. This procedure has been applied to the raw data points. A Lorentzian function was convoluted with an experimental Gaussian curve ($G = 0.8$) and a Shirley background (17) was subtracted. Then values of BE, γ (half-width at half maximum of the Lorentzian curve), and peak area were deduced. The relative element intensities (Pt, Zn, Cl) were calculated from peak surface ratio measurements, corrected by differences in escape depths (a root square approximation was used) and in cross-section (using Scofield's data (18)).

X-Ray Diffraction Analysis (XRD)

XRD analyses were carried out in a Siemens D 5000 polycrystalline diffractometer using Cu$K\alpha$ radiation. Some spectra were recorded in a rapid scanning mode (2.0 s/step, step size 0.05° in 2θ) in a large 2θ range (5°–100°). Such spectra showed all the lines of the zincite structure of ZnO (JCPDS 36-1451) and other lines characteristic of the Pt metal (JCPDS 4-0802) or the Pt–Zn alloy (JCPDS 6-0604); the other Pt_xZn_y phases reported in the literature (JCPDS 23-0466, 12-0612, 6-0619, and 6-0584) were not found. For better accuracy in the measurement of Pt and Pt–Zn lines, the spectra were recorded in the 38.5–42.5° 2θ range; this corresponds to the region of Pt and Pt–Zn (111) lines (respectively, 39.752 and 40.790), with 0.01° in step size and 5.0 s/step. The mean size of the particles (t) was related to the pure X-ray broadening using Scherrer's formula ($t = K\lambda/\varepsilon \cos\theta$, where $\lambda = 1.5406$ Å, ε = angular width at half-height expressed in radians, K = Scherrer constant (taken = 0.9 (19)), and θ = Bragg angle).

Temperature-Programmed Reduction (TPR)

The reducibility of the support and the catalysts was followed by TPR in a gas flow system with 1.5% H_2/Ar using an X-Sorb-(S) instrument (GIRA society). First, the sample (100 mg) was calcined in air at 673 K for 4 h, then cooled to room temperature and flushed with Ar (20 min), followed by a 1.5% H_2/Ar mixture (20 min); after this the TPR was performed, at 8 K/min until a temperature of 873 K was reached, where the sample was kept for 1 h.

RESULTS

When the catalytic test was performed under crotonaldehyde and H_2 constant flow, at constant temperature (353 K), the overall activity was found to decrease during the time on stream to reach a quasi steady state after about 2 h with a relatively fast and profound deactivation. This was observed with both A and B catalysts (Figs. 1A and 1B). In Table 2 are reported the activities and selectivities obtained in this quasi steady state after 2 h on stream. The A catalyst had the highest activity when reduced at 473 K; a further increase in the reduction temperature led to a decrease in the activity, but at 673 K both catalysts, A and B, showed nearly the same activity. The most remarkable result was the difference in selectivities obtained with the two catalysts. On the A catalyst, the crotyl alcohol selectivity was low after 473 K reduction (21%) and increased up to 45 and 49% after 573 and 673 K reduction. **On the B catalyst the crotyl alcohol selectivity reached a value as high as 75–80%, whatever the reduction temperature**. It could be noticed that some amounts of side products were formed, mainly on the B catalyst reduced at 573 K. An attempt was made to identify some of these using the GC mass coupling analysis. It revealed the presence of chlorinated products, the crotyl alcohol isomer, and dienic polymers. The production of these side products was constant during all the time on stream. The hydrocarbon analysis showed a mixture of butane, butenes, and butadiene. In Fig. 2 we reported the selectivities, recalculated by taking into account the direct hydrogenated products, butanal, CROTOL, butanol, and hydrocarbons, obtained on the B catalyst as a function of the time on stream. It is remarkable that these selectivities were independent of the reduction temperature. In the first minutes of the run, products from consecutive reaction, such as butanol and hydrocarbons, were formed in slightly higher quantities, giving then lower selectivity in CROTOL, but the latter stabilized very quickly at $82 \pm 3\%$. This high value was obtained in a conversion range going from 5 to 20%.

TABLE 2

Hydrogenation of Crotonaldehyde on 5% Pt/ZnO (A: Metal Precursor, $Pt(NH_3)_4(NO_3)_2$; B: Metal Precursor, H_2PtCl_6)

Catalyst	A			B		
T. red.	473	573	673	473	573	673
A (μmol/s/g of Pt)	7	1.8	1.5	4	3.3	1.6
	Selectivity					
HC	<1	<1	<1	1	1[a]	<2
Butanal	63	40	47	15	15	15
Butanol	15	12	4	1	1	<1
CROTOL	**21**	**45**	**49**	**78**	**75**	**81**
Side products	1	2	1	5	8[b]	2

[a] Butadiene, butenes, and butane.
[b] Chlorinated products (2–3%), CROTOL isomers (3–4%), and dienic polymer (1–2%).

The XRD results are reported in Figs. 3A and 3B in the 38.5–42.5 2θ range. On one hand, the A catalyst, calcined at 673 K or reduced at 473 K, showed similar Pt lines, characteristic of Pt metal; the particles can be estimated to 15 nm.

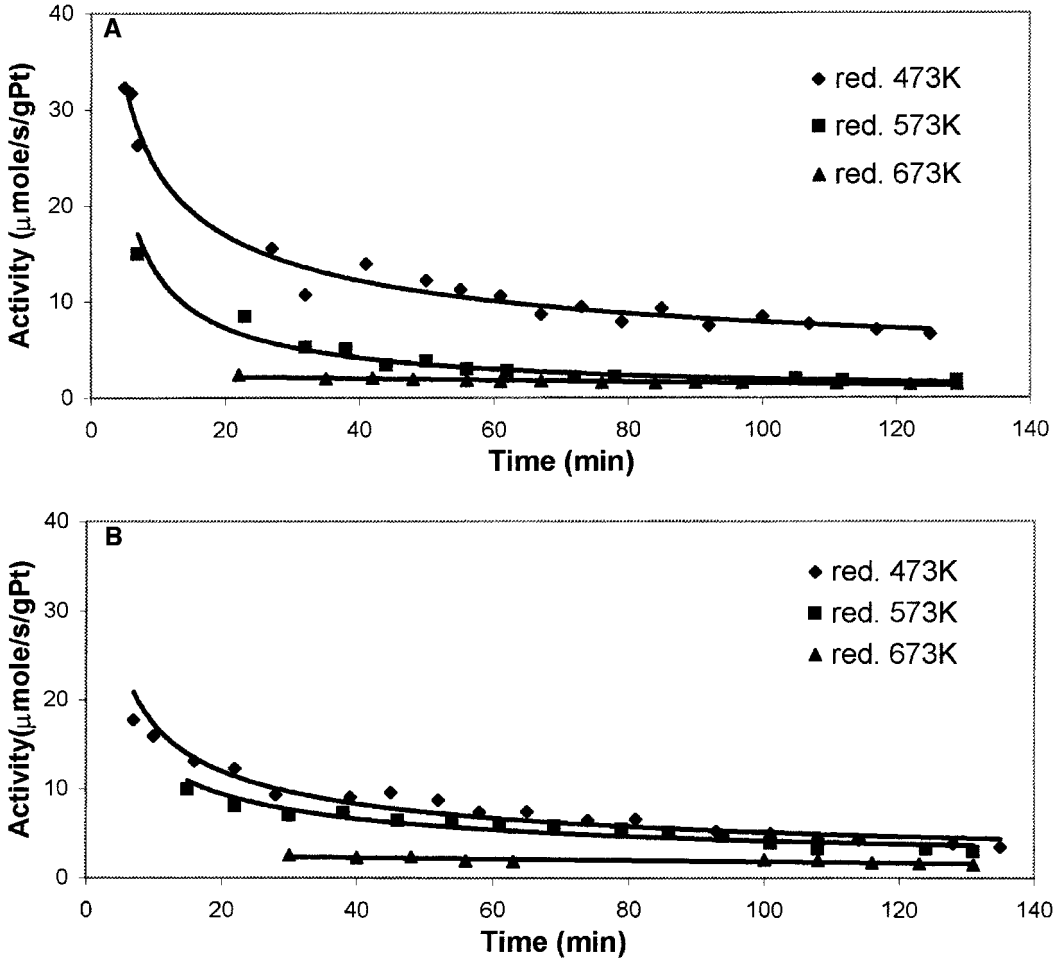

FIG. 1. (A) Hydrogenation of crotonaldehyde on 5% Pt/ZnO, A catalyst (metal precursor: $Pt(NH_3)_4(NO_3)_2$). (B) Hydrogenation of crotonaldehyde on 5% Pt/ZnO, B catalyst (metal precursor: H_2PtCl_6).

When the reduction temperature was increased to 573 K the Pt line intensity decreased while the Pt–Zn alloy line grew to become the most prominent line after 673 K reduction temperature, revealing the presence of 18-nm PtZn particles. On the other hand, with the B catalyst, reduced at 473 K, no line corresponding to Pt and PtZn was visible; it was only after 673 K reduction temperature that a well-defined line appeared, indicating the presence of PtZn particles, sized at 9 nm. After 473 K reduction temperature the metal particles were too small to give a diffraction pattern. Therefore, from XRD analysis, no conclusion can be drawn as to the nature of these particles at this low reduction temperature.

The XPS spectra showed no change in the binding energies and line shapes of all the XPS and XAES lines corresponding to the Zn element on both catalysts and whatever the reduction treatment, on the condition that the reduction temperature was less than 773 K. This result allowed us to take any Zn lines as an internal reference. It is only from the 773 K reduction treatment that we observed a beginning of ZnO reduction when the shape of the XAES lines was analyzed as described in the literature (11). For the Pt(4*f*) lines, an example of the curve fitting is shown in Fig. 4 and the quantitative results of all the samples are reported in Table 3. When the catalysts were reduced, there was no noticeable change in the binding energy as the reduction temperature increased; the (70.8 ± 0.1)-eV value of the binding energy corresponds to Pt in the reduced state. Differently, regarding the γ values, a narrowing of the line width was clearly observed for the A catalyst: γ decreased from 0.45 to 0.39 and 0.23 when the reduction temperature was increased from 473 K to 573 and 673 K, respectively. On the B catalyst, with a reduction temperature as low as 473 K, a low γ value (0.27) was obtained and decreased down to 0.23 for 673 K reduction temperature. In the calcined state, the peaks were not unique: in the A catalyst, the Pt lines corresponded mainly to the Pt metal (60%) while in the B catalyst 80% of Pt gave a component at 3.5 eV BE higher than the metal one. XPS studies of the oxygen–platinum (20) and chlorine–platinum (21) compounds reported in

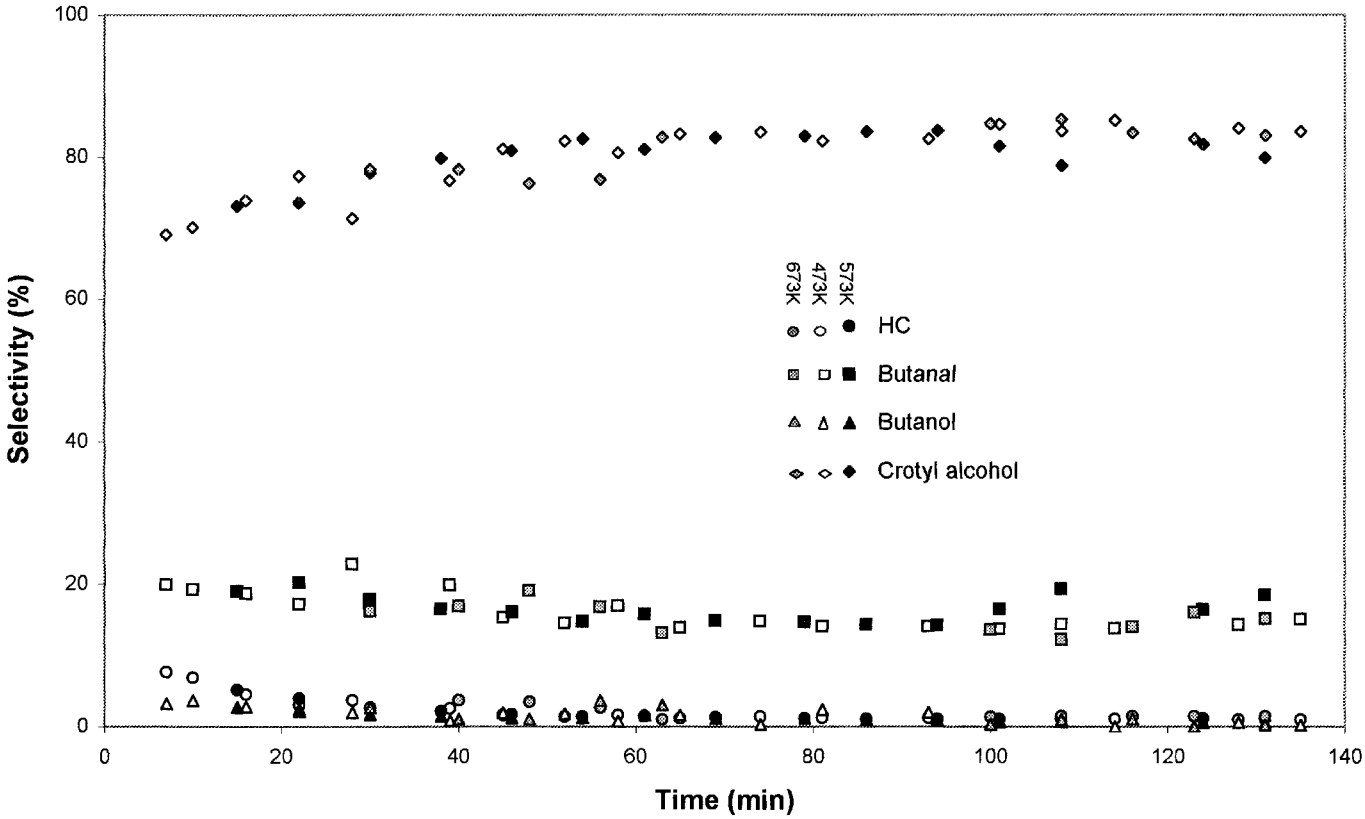

FIG. 2. Hydrogenation of crotonaldehyde on 5% Pt/ZnO, B catalyst (metal precursor: H_2PtCl_6) reduced at 473, 573, and 673 K.

the literature led us to assign the highest BE Pt component to a chlorinated or oxychlorinated compound rather than PtO_2 species since a large amount of chlorine remained on the surface as discussed below. The other secondary components in both catalysts were located between 1 and 2 eV higher than the metal one (72 and 72.4 eV) and should correspond to some PtO_x species, in which the Pt oxidation degree was hardly defined.

The (Pt/Zn) atomic ratios were about twice as high on the B catalyst as on the A catalyst, revealing a larger surface area of platinum on the B catalyst, meaning that smaller particles have been formed on B than on A; this result was in accordance with XRD analyses.

Chlorine was present in large amounts in the B catalyst, whatever the reduction temperature (between 5 and 7 times the number of platinum atoms). Small amounts of chlorine existed in the A catalyst after reduction at 473 K, which disappeared at 673 K reduction temperature, but one has to notice that the chlorine atoms were also present in the calcined ZnO support and in the same proportion

TABLE 3

XPS Analyses of Pt(4*f*) and Cl(2*p*) Lines

	BE ($Pt(4f)^{7/2}$) (eV)		γ (Pt(4*f*)) (Lorentzian half-width)		100 × (Pt/Zn) atomic ratio theoretical = 2.2		100 × (Cl/Zn) atomic ratio	
	A	B	A	B	A	B	A	B
Calc. at 673 K 4 h	70.7	72.0	0.50	0.37	1.2	0.9	7	22
	72.4	74.2	0.50	0.32	0.6	3.2		
Red. at 473 K 2 h	70.7	70.8	0.45	0.27	1.8	3.7	4	20
Red. at 573 K 2 h	70.7	70.7	0.39	0.25	1.8	3.7	2	19
Red. at 673 K 2 h	70.9	70.7	0.34	0.23	1.7	2.9	ε	14
Red. at 673 K 4 h	70.9	70.7	0.23	0.23	1.4	2.9	ε	19

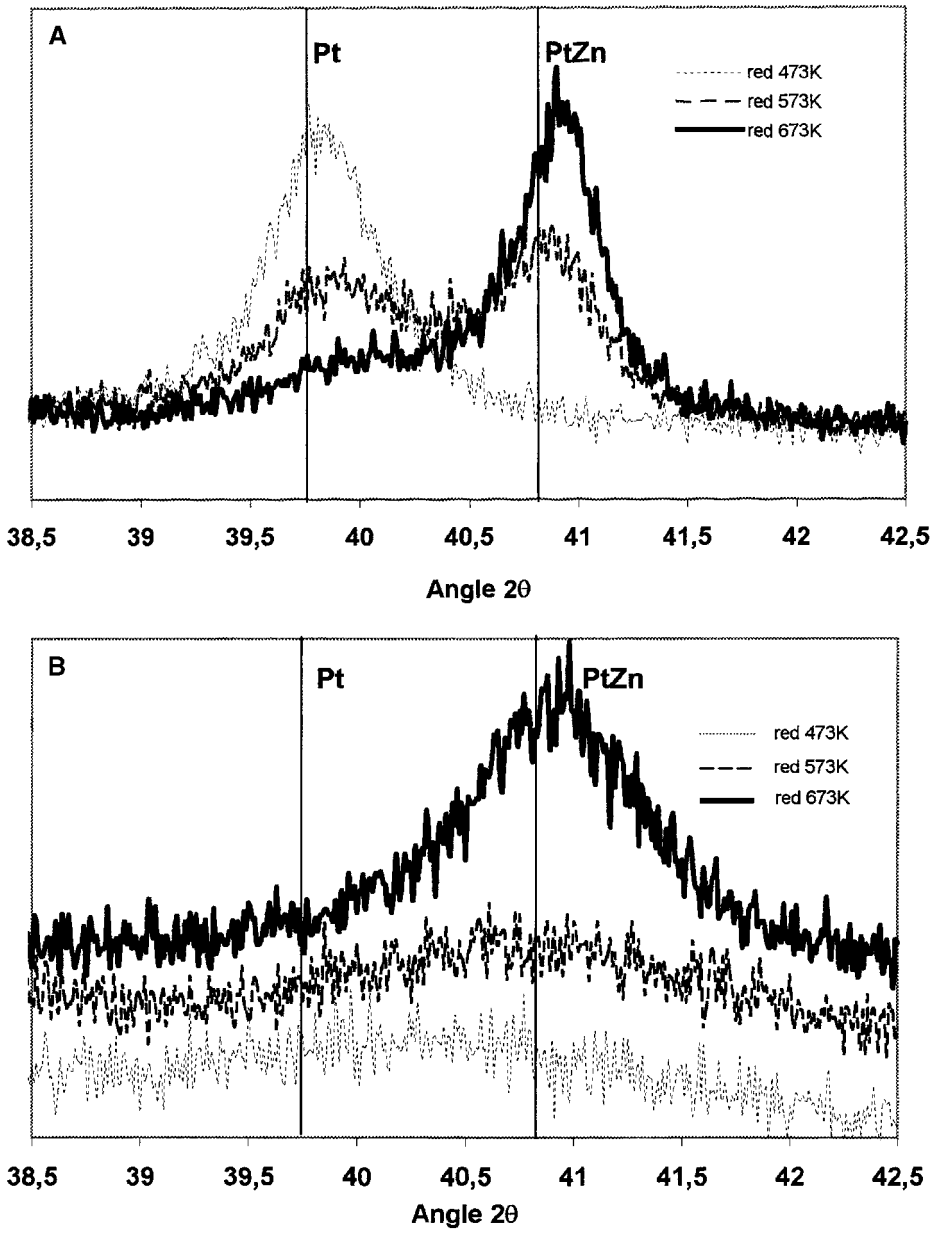

FIG. 3. (A) XRD analysis on 5% Pt/ZnO, A catalyst (metal precursor: $Pt(NH_3)_4(NO_3)_2$). (B) XRD analysis on 5% Pt/ZnO, B catalyst (metal precursor: H_2PtCl_6).

as that in the calcined A catalyst. The AAS analyses confirmed the results from XPS analyses, as can be seen from Table 1.

The TPR profiles of the A and B catalysts were totally different (Fig. 5). On the B catalyst a large peak of H_2 consumption appeared between 473 and 573 K with an H_2/Pt ratio equal to 3.3. In the Pt/Al_2O_3 systems, such a high-temperature reduction peak was usually assigned to the reduction of oxychlorinated platinum species (22). Moreover, a stoichiometry, $H_2/Pt = 3$, has already been found and attributed to the presence of $Pt(OH)_4Cl_2$ when chlorinated Pt/Al_2O_3 catalysts were concerned (23):

$$Pt(OH)_4Cl_2 + 3H_2 \rightarrow Pt + 4H_2O + 2HCl.$$

We could estimate that similar species were formed on this calcined H_2PtCl_6/ZnO catalyst, knowing that Cl atoms were present on the surface (from AAS and XPS analyses) and high BE was found for the Pt(4*f*) line in XPS. Different from the B catalyst, on the A catalyst a small consumption of H_2 occurred at 393 K, corresponding to H_2/Pt equal to 0.13. This suggested that the particles in this A catalyst were

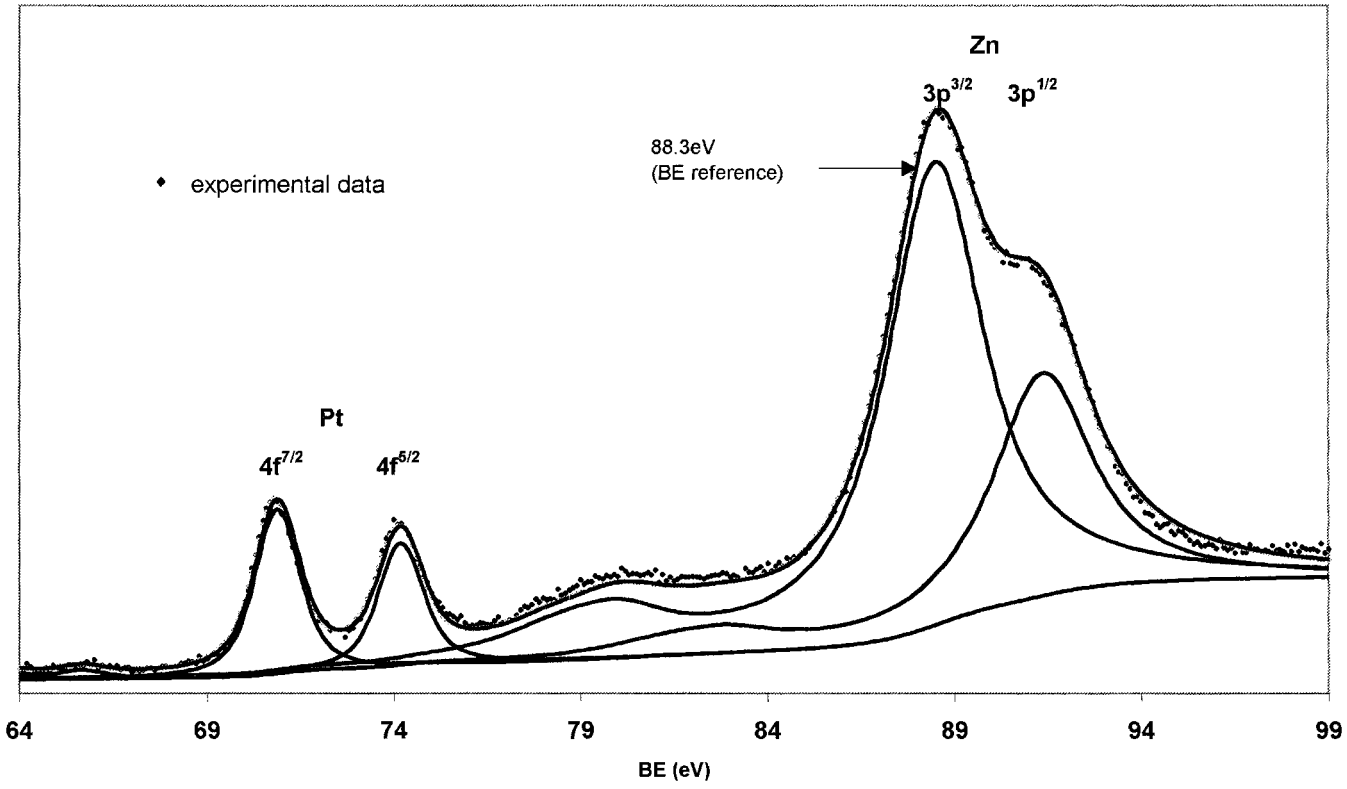

FIG. 4. XPS analysis, example of fit in Pt(4*f*)–Zn(3*p*) BE range (5% Pt/ZnO, B catalyst (metal precursor: H_2PtCl_6) reduced 4 h at 673 K).

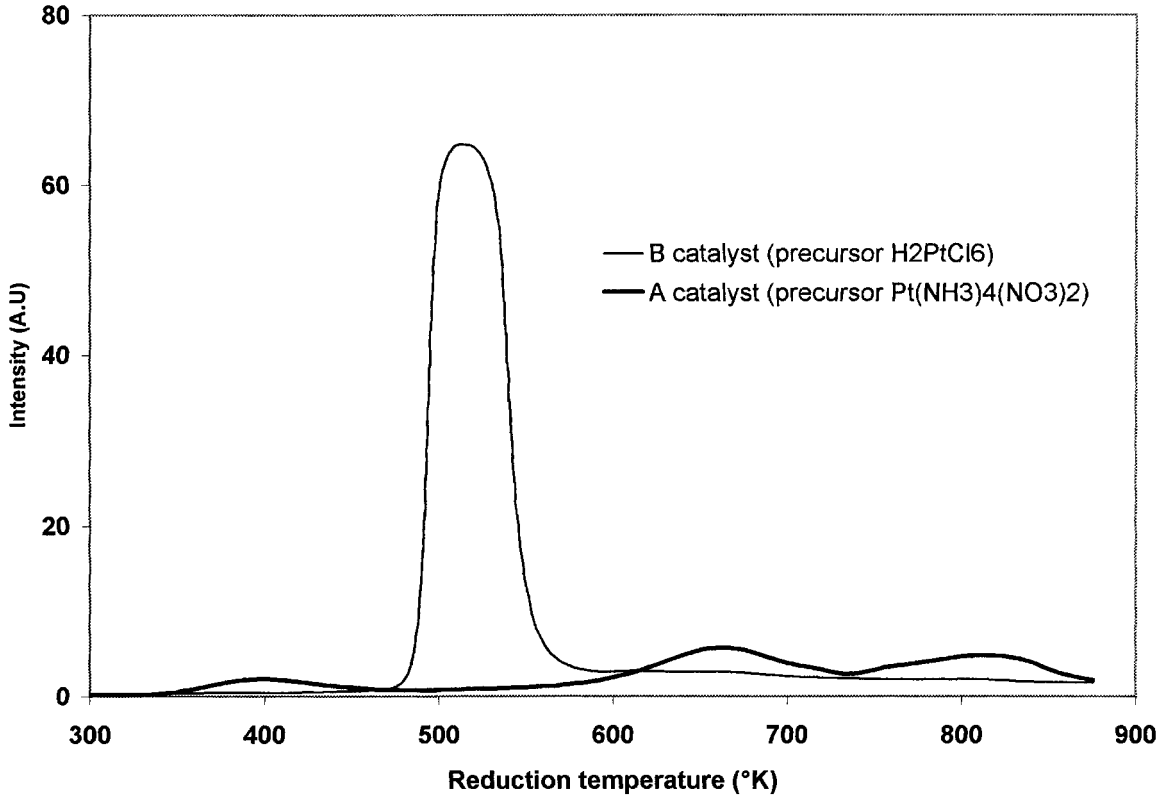

FIG. 5. TPR on 5% Pt/ZnO (after calcination at 673 K).

surrounded by platinum oxide while the bulk was formed of platinum metal, as already reported in the literature (24). Moreover, this result corroborated the preceding analyses by XRD and XPS: the XRD spectrum, representative of the particle bulk, revealed the presence of Pt metal for the calcined A catalyst while XPS results in which the contribution of the surface was important showed both oxide and metal platinum on the A catalyst and only chlorinated species on the B catalyst. The reduction of ZnO on the A catalyst was apparent between 523 and 873 K with two maxima at 658 and 813 K. A part of the reduced Zn was engaged in the Pt–Zn alloy formation. This phenomenon also occurred on the B catalyst since the baseline after the platinum species reduction peak had not recovered the zero level, indicating that a continuous reduction process occurred; moreover, in the 473–573 K temperature range the excess hydrogen which is not involved in the reduction of $Pt(OH)_4Cl_2$ ($H_2/Pt > 3$) is used for the reduction of ZnO to form the PtZn alloy.

DISCUSSION

Deactivation

Experimental data on selectivity dependence on time on stream (Fig. 3) showed that, for the B catalyst, the selectivities, measured in the 5–20% conversion range, were independent of the reduction temperature pretreatments and then of the activities.

As we pointed out (25), from a kinetic point of view, such a behavior implies that deactivation phenomena and complex reaction kinetics can be treated separately. Similarly to our previous consideration (25) one can speculate that catalyst decay, at least for the B catalyst, is due to the formation of coke deposits from the starting products parallel to the main hydrogenation reaction. We assume that coke (or carbon deposit) is produced from adsorbed crotonaldehyde. Deactivation and self-regeneration proceed simultaneously; moreover, these steps are essentially slower than the reaction steps. This consideration allows one to apply a steady-state hypothesis only to hydrogenation but not to the deactivation steps. A detailed kinetic analysis was presented in (25). Here, we present only the final equation for the reaction rate,

$$r = a_3 + a_1 \exp(-a_2 t), \qquad [1]$$

where

$$a_1 = k_s r_0/(k_s + k_{-s}); \quad a_2 = k_s + k_{-s}; \quad a_3 = k_{-s} r_0/(k_s + k_{-s}). \qquad [2]$$

Here, k_s and k_{-s} denote the deactivation and self-regeneration rate constants and r_0 the rate in deactivation-free conditions.

Equation [1] was used for fitting experimental data. The sum of squares of the relative deviations served as an object function. Results of the simulations are presented in Table 4; $a_1 + a_3$ represents the initial rate and a_3 the rate at infinite time. It is worth noting that the B catalyst, after reduction at 473 K, retains significant activity at infinite time, knowing that it shows an exceptional crotyl alcohol selectivity.

TABLE 4

Kinetic Parameters in the Deactivation Process ($r = a_3 + a_1 \exp(-a_2 t)$)

Catalyst	a_1	a_2	a_3	ss[a]
A, 473 K	31.31 ± 1.57	0.041 ± 0.004	6.99 ± 0.63	0.99
A, 573 K	18.53 ± 0.65	0.047 ± 0.003	1.73 ± 0.19	0.13
A, 673 K	1.74 ± 0.14	0.024 ± 0.004	1.38 ± 0.06	0.003
B, 473 K	16.80 ± 1.20	0.029 ± 0.006	3.99 ± 1.00	0.49
B, 573 K	10.10 ± 2.50	0.011 ± 0.007	0.70 ± 3.16	0.42
B, 673 K	2.54 ± 0.27	0.003 ± 0.001	0	0.033

[a] Sum of squares of the relative deviations.

Kinetics

For further discussion let us briefly analyze the reaction network and reaction kinetics. The kinetic network was originally proposed by Simonik and Beranek (26) and further developed in (6). In the original treatment of Simonik and Beranek, isomerization from crotyl alcohol into butyraldehyde was assumed. In (25), we even supposed that the opposite isomerization reaction from butyraldehyde into crotyl alcohol takes place, due to specific features of the support which was applied and hence to the reactivity of the C=O bond. However, calculations in (25) showed that this isomerization step can be neglected. In the present paper for the more general treatment we assume that the isomerization step is reversible. The kinetic considerations in (6) were somewhat simplified, as it was assumed that there exists only one equilibrium constant for crotonaldehyde adsorption. However, this molecule can be adsorbed by an olefinic bond as well as by a C=O bond. Moreover, both unsaturated bonds can be bounded to the metal surface, enhancing crotonaldehyde adsorption by the resonance effect (delocalization of electron density).

The reaction network is presented in the following scheme:

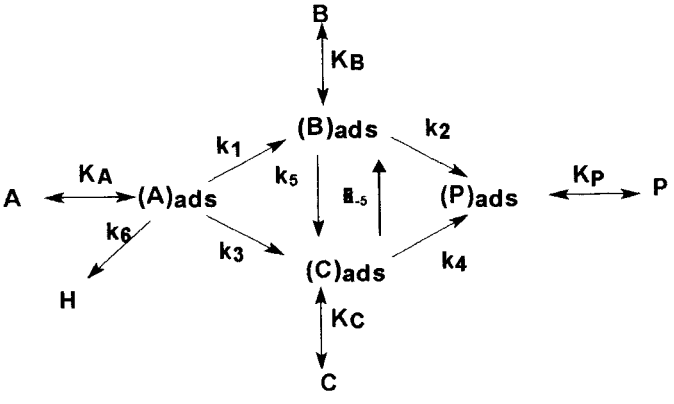

The proposed reaction mechanism is

	$N^{(1)}$	$N^{(2)}$	$N^{(3)}$	$N^{(4)}$	$N^{(5)}$	$N^{(6)}$	$N^{(7)}$
(K_{AB})							
1. $Z + A \equiv ZA_B$	1	0	0	0	0	0	0
k_1							
2. $ZA_B + H_2 \rightarrow B + Z$	1	0	0	0	0	0	0
(K_{AC})							
3. $Z + A \equiv ZA_C$	0	1	0	0	0	0	0
k_3							
4. $ZA_C + H_2 \rightarrow C + Z$	0	1	0	0	0	0	0
(K_{ABC})							
5. $Z + A \equiv ZA_{BC}$	0	0	1	1	0	0	0
k_1							
6. $ZA_{BC} + H_2 \rightarrow ZB$	0	0	1	0	0	0	0
(K_B)							
7. $ZB \equiv Z + B$	0	0	1	0	-1	0	1
k_3							
8. $ZA_{BC} + H_2 \rightarrow ZC$	0	0	0	1	0	0	0
(K_C)							
9. $ZC \equiv Z + C$	0	0	0	1	0	-1	-1
k_2							
10. $ZB + H_2 \rightarrow ZP$	0	0	0	0	1	0	0
k_4							
11. $ZC + H_2 \rightarrow ZP$	0	0	0	0	0	1	0
(K_P)							
12. $ZP \equiv Z + P$	0	0	0	0	1	1	0
k_5							
13. $ZC \leftrightarrow ZB$	0	0	0	0	0	0	1
k_{-5}							

$N^{(1)}$, $N^{(3)}$: $A + H_2 \rightarrow B$
$N^{(2)}$, $N^{(4)}$: $A + H_2 \rightarrow C$
$N^{(5)}$: $B + H_2 \rightarrow P$
$N^{(6)}$: $C + H_2 \rightarrow P$
$N^{(7)}$: $C \rightarrow B$

Here, A, B, C, and P denote crotonaldehyde, butyraldehyde, crotyl alcohol (desired product), and butanol, respectively. A_B represents adsorption of crotonaldehyde via an olefinic bond, A_C via the carbonyl bond, and A_{BC} via both bonds, respectively. Steps 2, 4, etc. are not necessarily elementary reactions; they can consist of several elementary reactions with only one of them being rate-determining. In the above mechanism, Z is a surface site. On the right-hand side of the equations of steps, stoichiometric numbers (27, 28) for the different routes ($N^{(1)}$, etc.) are given.

In addition to these reaction steps, there exist also deactivation steps, however these are not depicted in this mechanism. Here, we can only speculate about the types of adsorbed species which lead to side products. Hydrocarbons and dienic polymers can arise from adsorbed crotonaldehyde, while chlorinated products can be formed from any adsorbed species.

Experimental data on selectivity show clearly that the selectivity patterns for crotyl alcohol and butyraldehyde follow similar trends; therefore, the isomerization reaction between these molecules can be neglected in kinetic modeling. Deriving kinetic equations from the mechanism above (and neglecting isomerization step 13), one arrives at the following equations which relate the selectivities toward B and C,

$$S_B = dP_B/dP_A = L_B - M_B P_B/P_A, \quad [3]$$

$$S_C = dP_C/dP_A = L_C - M_C P_B/P_A, \quad [4]$$

where

$$L_C = \frac{1}{1 + k_1'(K_{AB} + K_{ABC})/k_3'(K_{AC} + K_{ABC})}, \quad [5]$$

$$L_B = 1 - L_C, \quad [6]$$

and

$$M_C = L_C \frac{k_4'}{k_3'(1 + K_{ABC}/K_{AC})}, \quad [7]$$

$$M_B = L_B \frac{k_2'}{k_1'(1 + K_{ABC}/K_{AB})}. \quad [8]$$

Constants k_1' are effective, as they contain hydrogen pressure dependence. Constants of equilibrium steps are related to adsorption/desorption coefficients

$$K_{AB} = \frac{k_{AB}}{k_{-AB}}; \quad K_{AC} = \frac{k_{AC}}{k_{-AC}}; \quad K_{ABC} = \frac{k_{AB} + k_{AC}}{k_{-AB} + k_{-AC}}. \quad [9]$$

An analysis of Eqs. [3] and [4] reveals that the initial selectivity (at low conversions) depends on the L_C value. The selectivity profile as a function of conversion depends more on the M_C value. For parallel-consecutive reactions the lower the value of M_C, the less pronounced is the C selectivity dependence on the conversion.

It is quite clear from Eq. [5] that the L_C value depends on both kinetic (k_1/k_3) and adsorption factors $(K_{AB} + K_{ABC})/(K_{AC} + K_{ABC})$.

It follows from the literature and from our own experimental data that the selectivity in crotyl alcohol strongly depends on the type of support as well as on the reduction temperature for the case of reducible supports. It is also evident that in some cases an increase in selectivity is associated with a decrease in activity (A catalyst, for example). On one hand, however, as with the B catalyst, although the selectivity is almost independent of the reduction temperature, the overall activity in hydrogenation varied. On the other hand, at exactly the same overall activity for the A and B catalysts, the selectivities differed dramatically. Although the kinetic factor does not represent the overall catalytic activity but rather the ratio of hydrogenation constants of olefinic and carbonyl bonds, it seems feasible to speculate that the kinetic factor is less dependent than the adsorption factor on the type of support.

Promotion Mechanism

Experimental data on crotonaldehyde hydrogenation show a very strong influence of the catalyst support on the

reaction selectivity. Potential promotion effects in the hydrogenation of α,β-unsaturated aldehydes were analyzed by Ponec (3). Promoters were defined as nonmetallic additives which, being inactive by themselves, influence the activity and the selectivity:

(1) If the nonmetallic additive is reduced, it can form an alloy with the main metal and then beneficial effects can be due to ensemble size effects, ensemble composition effects, and ligand or electronic influences.

(2) The ionic compounds could influence the surface composition of the support.

(3) There could be changes in the morphology and the size of the particles on a support.

(4) Promotion can also be of a chemical origin.

(5) Promoters can influence the accessibility of the special sites.

According to Ponec (3), a promoter should activate the carbonyl group, but not bind the olefinic group. The most likely explanation is that a positively charged cationic site is formed, leading to the formation of the following species:

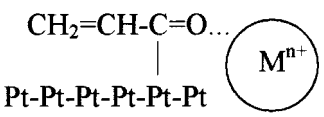

Recently, the influence of metal cations on the selective hydrogenation of α,β-aldehydes (cinnamaldehyde and crotonaldehyde) over polymer-stabilized platinum colloid was studied. Yu *et al.* (29) added metal cations after the formation of a colloidal platinum catalyst, diminishing the possibility of influencing the size, shape, or structure of metal colloidal particles. The addition of Fe^{3+} and Co^{2+} increased both the activity and the selectivity in crotonaldehyde hydrogenation. A slight increase in selectivity was observed when Zn^{2+} was added to the Pt–Fe^{3+} system; moreover, the activity decrease and the selectivity increase could be correlated with the amount of added Zn^{2+}. The mechanism of the modification of metal cations to the Pt colloid (M = Fe, Co, Ni, etc.) given by Yu *et al.* is presented below:

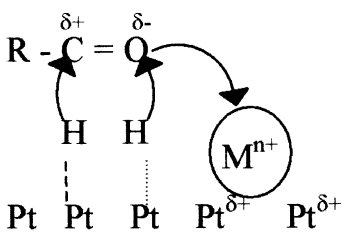

Let us discuss our own experimental data, taking as a basis the considerations addressed above.

The Pt/ZnO catalysts prepared from $Pt(NH_3)_4(NO_3)_2$ (A) and H_2PtCl_6 (B) differentiate each other by the physical characteristics and by the catalytic behavior as well.

The B catalyst was much better dispersed than the A catalyst, certainly due to the formation of oxychlorinated species during the calcination step.

The noble metal in the catalyst formed an alloy with Zn. A reduction temperature as high as 573 K was necessary for the A catalyst to form an alloy. That was clearly shown from XRD spectra and could also be deduced from XPS analyses in which the narrowing of the Pt 4*f* lines occurred parallel to the increase in the reduction temperature and then to the alloy formation. In fact, the line width in the XPS line is related to the electronic structure as it was already observed in PdPb (30) or PdSb (31) alloys. Since we observed a narrow Pt(4*f*) line for the B catalyst after 473 K reduction temperature, we can conclude that the alloy has already been formed at this low reduction temperature.

On the A catalyst, after 473 K reduction, the catalytic behavior of Pt metal particles dispersed on ZnO showed low selectivity in crotyl alcohol; however, when the reduction temperature is increased, one observes, parallel to the formation of the PtZn alloy, a decrease in activity and an increase in crotyl alcohol selectivity. It is tempting to conclude that the Pt sites, when alloying to Zn, form $Pt^{\delta-}$–$Zn^{\delta+}$ entities. These entities would not adsorb the crotonaldehyde molecule by binding to the olefinic bond but rather by binding to the carbonyl bond. In fact, if the Pt atom is electron-rich, it repels the electrons of the C=C bond while it is attracted by the electropositive carbon of the C=O bond and the electronegative oxygen atom is bonded to the electropositive Zn atom. Such a charge transfer could be too small to be revealed by a Pt(4*f*) binding energy shift; however, it has already been suggested by Li *et al.* (11) and by Boccussi *et al.* (32).

Besides this alloying effect, it is clear that chlorine has a promotor effect in this reaction since when both catalysts contain quasi exclusively Pt–Zn particles, after 673 K reduction, the B catalyst gives a much higher crotyl alcohol selectivity (80%) than the A catalyst (50%) with similar activity. The difference in particle sizes (9 nm for B and 18 nm for A) can hardly be invoked to explain the different catalytic behaviors. Nitta *et al.* (33) have also found a promotor effect of chlorine in the unsaturated alcohol selectivity in the hydrogenation of α,β-unsaturated aldehydes on cobalt catalysts. They concluded that the residual chlorine in these catalysts affected both, the H_2-reduction step leading to a "favorable" crystallite size distribution and the reaction stage depressing more strongly the C=C bond than the C=O bond hydrogenation reaction. Yu *et al.* (34) supposed that the Cl^- anion acted only as spectator ions in crotonaldehyde hydrogenation. The possible influence of Cl^- ions was not mentioned in the review of Ponec (3), probably due to the common belief that chloride acts merely as a poison. However, some examples exist showing the promotion effect of Cl^- in heterogeneous catalytic reactions. For instance, the ethylene oxidation process was strongly influenced by the chloride ions (35, 36); a decrease

of oxygen adsorption on the silver catalysts was observed with the increase of the chloride-covered fraction of the surface. It was believed that Cl^- ions diminished the rate of undesired reaction, e.g., total oxidation, thus promoting the main reaction—ethylene oxide formation. It was observed that, at lower chloride concentrations, catalytic activity even increased, while poisoning effects were observed only at higher Cl^- concentrations. Electronic and geometric effects were thought to be responsible. Recently, it was shown that modification of nickel catalysts by impregnation with chlorine-containing compounds led not only to a decrease in the overall catalytic activity in thymol (3-methyl-6-isopropylphenol) hydrogenation but also to changes in selectivity. The latter was attributed to alteration of keto–enol transformations of intermediate menthones and corresponding enols (37).

In light of our previous considerations, we can speculate that Cl^- remaining in the catalyst after reduction can polarize even stronger $Zn^{\delta+}$, increasing therefore the interactions between $Zn^{\delta+}$ and $O^{\delta-}{=}C$, thus increasing the equilibrium constant of crotonaldehyde adsorption via the C=O bond. In terms of Eq. [5] this means that there is an increase of the K_{AC} value, leading under certain conditions to the overall decrease of the second term in the denominator.

Let us make simple calculations neglecting the diadsorbed mode of crotonaldehyde and assuming that the kinetic factor is constant, whatever the experiment presented here ($K_{ABC} = 0$, $(k'_m/k'_n)^* = (k'_m/k'_n)^{**}$ where * and ** represents two sets of experiments). One arrives at

$$\frac{(K_{AC}/K_{AB})^*}{(K_{AC}/K_{AB})^{**}} = \frac{(1 - L_C^{**})}{(1 - L_C^*)} \frac{L_C^*}{L_C^{**}}.$$

This means that taking the different selectivities 50 and 80%, observed respectively for A and B catalysts, reduced at 673 K, the ratio of adsorption constants is four times higher on B catalysts containing chlorine than on A catalysts.

CONCLUSION

Catalyst A, 5% Pt/ZnO prepared from $Pt(NH_3)_4(NO_3)_2$ which does not contain Cl^-, displays more or less conventional mechanisms, typical of platinum deposited on reducible supports in which one can assume alloy formation and/or migration of reducible oxide onto the metal particles like in Pt/TiO_2 catalysts. For such catalysts, which display modest crotyl alcohol selectivity in crotonaldehyde hydrogenation, there is a correlation between reduction temperature, decrease in activity, and increase in C=O bond hydrogenation selectivity. On the contrary, the B catalyst, 5% Pt/ZnO prepared from H_2PtCl_6, contains Cl^- ions at any reduction temperatures, from 473 to 673 K. It forms a Pt–Zn alloy, even at low reduction temperature (473 K), and then shows one of the best selectivities to crotyl alcohol achieved so far in gas-phase crotonaldehyde hydrogenation (80% crotyl alcohol selectivity in 5–20% conversion range) with a significant and stable activity along the time of stream after a short period of initial deactivation.

REFERENCES

1. Augustine, R. L., "Heterogeneous Catalysis in Organic Synthesis." Dekker, New York, 1995.
2. Touroude, R., *J. Catal.* **65**, 110 (1980).
3. Ponec, V., *Appl. Catal. A* **149**, 27 (1997).
4. Margitfalvi, J. L., Tompos, A., Kolosova, I., and Valyon, J., *J. Catal.* **174**, 246 (1998).
5. Sen, B., and Vannice, M. A., *J. Catal.* **113**, 52 (1988).
6. Makouangou, R. M., Murzin, D. Yu, Dauscher, A. E., and Touroude, R. A., *Ind. Eng. Chem. Res.* **33**, 1881 (1994).
7. Englisch, M., Jentys, A., and Lercher, J. A., *J. Catal.* **166**, 25 (1997).
8. Claus, P., Schimpf, S., Schödel, R., Kraak, P., Mörke, W., and Hönicke, D., *Appl. Catal. A* **165**, 429 (1997).
9. Yoshitake, H., and Iwasawa, Y., *J. Chem. Soc., Faraday Trans.* **88**(3), 503 (1992).
10. Sepulveda-Escribano, A., Coloma, F., and Rodriguez-Reinoso, F., *J. Catal.* **178**, 649 (1998).
11. Li, W., Chen, Y., Yu, C., Wang, X., Hong, Z., and Wei, Z., *in* "Proceedings, 8th International Congress on Catalysis, Berlin, 1984," Vol. 5, p. 205. Dechema, Frankfurt-am-Main, 1984.
12. Boccuzzi, F., Chiorino, A., Ghiotti, G., Pinna, F., Strukul, G., and Tessari, R., *J. Catal.* **126**, 381 (1990).
13. Sarkany, A., Zsoldos, Z., Furlong, B., Hightower, J. W., and Guczi, L., *J. Catal.* **141**, 566 (1993).
14. Takezawa, N., and Iwasa, N., *Catal. Today* **36**, 45 (1997).
15. Iwasa, N., Masuda, S., Ogawa, N., and Takesawa, N., *Appl. Catal. A* **125**, 145 (1995).
16. Cubeiro, M. L., and Fierro, J. L. G., *J. Catal.* **179**, 150 (1998).
17. Shirley, D. A., *Phys. Rev. B* **5**, 4907 (1972).
18. Scofield, J. H., *J. Electron Spectrosc. Relat. Phenom.* **8**, 129 (1976).
19. Klug, H. P., and Alexander, L. E., "X-ray Diffraction Procedure for Polycrystalline and Amorphous Materials," 2nd ed. Wiley, New York, 1974.
20. Hecq, M., Hecq, A., Delrue, J. P., and Robert, T., *J. Less Common Meta.* **64**, P25 (1979).
21. Escard, J., Pontvianne, B., Chenebaux, M. T., and Cosyns, J., *Bull. Soc. Chim. Fr.* **11–12**, 2399 (1976).
22. Lieske, H., Lietz, G., Spindler, H., and Volter, J., *J. Catal.* **81**, 8 (1983).
23. Le Normand, F., Borgna, A., Garetto, T. F., Apesteguia, R., and Moraweck, B., *J. Phys. Chem.* **100**, 9068 (1996).
24. McCabe, R. W., Wong, C., and Woo, H. S., *J. Catal.* **114**, 354 (1988).
25. Consonni, M., Touroude, R., and Murzin, D. Yu, *Chem. Eng. Technol.* **21**, 7 (1998).
26. Simonik, J., and Beranek, L., *Collect. Czech. Chem. Commun.* **37**, 353 (1972).
27. Horiuti, J., *Res. Inst. Catal. Hokkaido Univ.* **5**, 1 (1957).
28. Temkin, M. I., *Adv. Catal.* **28**, 173 (1979).
29. Yu, W., Liu, H., Liu, M., and Tao, Q., *J. Mol. Catal.* **138**, 273 (1999).
30. Goetz, J., Volpe, M. A., Sica, A. M., Gigola, C. E., and Touroude, R., *J. Catal.* **167**, 314 (1997).
31. Van Attekum, P. M. Th., and Trooster, J. M., *J. Phys.* **9**, 2287 (1979).
32. Boccuzzi, F., Chiorino, A., and Guglielminotti, E., *Surf. Sci.* **368**, 264 (1996).
33. Nitta, Y., Hiramatsu, Y., and Imanaka, T., *J. Catal.* **126**, 235 (1990).
34. Yu, W., Liu, H., and Tao, Q., *Chem. Commun.* 1773 (1996).
35. Kul'kova, N. V., Kamenski, D., and Bonchev, D., *React. Kinet. Catal. Lett.* **7**, 335 (1977).
36. Campbell, C. T., and Koel, B. E., *J. Catal.* **92**, 272 (1985).
37. Allakhverdiev, A. I., Kul'kova, N. V., and Murzin, D. Yu., *Catal. Lett.* **29**, 57 (1994).